Journal of Molecular Graphics and Modelling 27 (2008) 421–429

Contents lists available at ScienceDirect

Journal of Molecular Graphics and Modelling

journal homepage: www.elsevier.com/locate/JMGM

Molecular mechanism for the effects of trehalose on β-hairpin folding revealed by molecular dynamics simulation

Fu-Feng Liu, Xiao-Yan Dong, Yan Sun *

Department of Biochemical Engineering, School of Chemical Engineering and Technology, Tianjin University, Tianjin 300072, China

ARTICLE INFO

Article history:
Received 18 April 2008
Received in revised form 20 July 2008
Accepted 22 July 2008
Available online 30 July 2008

Keywords:
Molecular simulation
Osmolyte
Peptide folding
Free energy landscape
Hydrogen bond

ABSTRACT

Recent work has shown that trehalose can facilitate and inhibit protein folding, but little is known about the molecular basis of these effects. Molecular-level insights into how the osmolyte affects protein folding are of significance for the rational design of small molecular additives for enhancing or hindering the folding of proteins. To investigate the molecular mechanisms of the facilitation and inhibition effects of trehalose on protein folding, molecular dynamics (MD) simulation of a β-hairpin peptide (Trp-Arg-Tyr-Tyr-Glu-Ser-Ser-Leu-Glu-Pro-Glu-Pro-Asp) in different trehalose concentrations (0–0.26 mol/L) is performed using an all-atom model. It is found that at a proper trehalose concentration (0.065 mol/L), the peptide folds faster than that in water, but it cannot fold to the β-hairpin at higher trehalose concentrations. Free energy landscape analysis indicates the presence of three intermediate states in both pure water and in 0.065 mol/L trehalose, but the potential energy barriers in the folding pathway decrease greatly in 0.065 mol/L trehalose, so the peptide folding is facilitated. Moreover, at this trehalose concentration, there is a favorable balance between the peptide backbone hydrogen bonds (H-bonds) and the peptide-trehalose H-bonds, leading to the stabilization of the folded peptide. At higher trehalose concentrations, however, trehalose molecules cluster in the peptide region and interact with the peptide via many H-bonds that prevent the peptide from folding to its native structure. The energy landscape analysis indicates that the potential energy barriers increase so greatly that the peptide cannot overcome it, getting trapped in a local free energy basin. The work reported herein has elucidated the molecular mechanism of the peptide folding in the presence of trehalose.

1. Introduction

Osmolytes are small organic compounds that are ubiquitous in living systems. Osmolyte molecules in aqueous solution can have profound effects on protein stability, structure, and function [1], and it has long been known that osmolytes as solvent additives have significant effects on protein folding or unfolding [2]. Recently, various osmolytes such as trimethylamine N-oxide [3], glycerol [4], betaine [5] and trehalose [6] were used to study protein folding experimentally. Among the osmolytes, trehalose, a disaccharide produced by a wide variety of organisms, has received special interest because it possesses particular physicochemical and biological properties [7,8]. Trehalose molecules in aqueous solution can exert a dramatic influence on protein folding reactions. It was observed that trehalose showed an extraordinary capability to assist folding from denatured to native-like species [9]. Singer and Lindquist [10] found experimentally that trehalose could enhance and inhibit protein folding, and the favoring and inhibiting effects of trehalose on protein folding depended on its concentration. Despite its widespread use, the molecular basis for trehalose's ability to assist and inhibit protein folding remains unknown. Some direct interaction models have been suggested that trehalose binds to a folding protein by hydrogen bonds (H-bonds), leading to the stabilization of the folded state. The stabilizing effect shifts the equilibrium toward the native state, thereby favors the protein folding [11]. It has also been proposed that trehalose indirectly influences protein folding by being preferentially excluded from the backbone of the protein, which raises the free energy of the unfolded state and favors the folded population [12]. However, these interpretations do not provide molecular details for the folding pathway on how the protein overcomes the potential energy barrier to fold into its native state.

Molecular-level insights into how trehalose molecules facilitate or inhibit protein folding would be invaluable for the rational

* Corresponding author. Tel.: +86 22 27404981; fax: +86 22 27406590.
E-mail address: ysun@tju.edu.cn (Y. Sun).

1093-3263/$ – see front matter © 2008 Elsevier Inc. All rights reserved.
doi:10.1016/j.jmgm.2008.07.002

design of small molecular additives for enhancing or hindering the folding of proteins. However, it seems unlikely that experimental approaches can provide the molecular details. Molecular simulation is expected to contribute greatly to this end.

Molecular dynamics (MD) simulation is one of the most popular computational tools that can provide direct information on protein folding processes [13]. Up to now, MD simulation has been performed at various levels of complexity, ranging from lattice models and Ğo models to fully atomic simulations with implicit or explicit solvent [14]. It can be used to supplement experiment and fill in some of the gaps in our knowledge about protein folding pathways and intermediates, which are often inaccessible from the current most sophisticated experimental approaches. For example, Bennion and Daggett [15] have applied MD simulation to depict the molecular basis for the chemical denaturation of proteins by urea.

Guided by the energy landscape theory, an understanding of the fundamental principles of protein folding has recently advanced due to the development of small fast-folding peptide systems, which are tractable to study by all-atom simulations [16]. Their small sizes relative to proteins make them more amenable to detailed experimental analyses and computational treatments with atomic models [17]. Recently, there have been many experiments and computer simulations that provide insight into peptide folding mechanisms [18]. Among the various peptide models, the β-hairpin peptide, a small protein structure motif with basic physics of protein folding, is often used. The kinetics of β-hairpin formation can provide information on the early events in protein folding [19,20]. Hence, an understanding of its folding mechanism in the presence of osmolytes will shed some light on protein folding pathways in osmolyte solutions.

Here, we report the MD simulation of the effect of trehalose molecules on the folding of the β-hairpin peptide starting from the fully extended structure in low trehalose concentrations (0.065–0.26 mol/L). Atomic details revealed in the simulation allow us to investigate the free energy landscape and the free energy changes during the folding at different trehalose concentrations. Analysis of the contribution of the H-bond interactions revealed from the simulation would give the molecular-level insight into the effect of the osmolyte on protein folding.

2. Methods

2.1. Molecular dynamics simulations

All MD simulations were performed using the GROMACS 3.3 program [21] together with the GROMOS96 force field [22] for each of the simulations. Water was modeled by the simple point charge (SPC) model [23]. Initial velocities were assigned according to a Maxwell distribution at 300 K. The MD simulations were carried out with a constant number of particles (N), pressure (P), and temperature (T), i.e., NPT ensemble. A non-bond pair list cutoff of 9.0 Å was used, and the pair list was updated every four time steps. The long range electrostatic interactions were treated with the particle mesh Ewald method [24]. Bond lengths were constrained using the LINCS algorithm [25]. A 2 fs time step was used to integrate the equations of motion with the Verlet leapfrog algorithm [26]. The calculations were carried out at 300 K and were coupled to a Berendsen bath with a coupling constant of 0.1 ps, whereas the pressure was coupled to 1 bar with a constant of 0.5 ps and a compressibility of 1.5×10^{-5} bar^{-1} [27]. For all simulations, the atomic coordinates were saved every 0.5 ps for subsequent analysis.

2.2. Molecular systems

The starting structure of the linear peptide with sequence Trp-Arg-Tyr-Tyr-Glu-Ser-Ser-Leu-Glu-Pro-Glu-Pro-Asp was constructed using the Discovery Studio v1.7 program (Accelrys, Inc.). We chose the peptide because previous MD simulations have shown that the peptide can easily fold to its native conformation of β-hairpin on a 6 ns time scale in explicit water [28]. Therefore, it permits a complex simulation with explicit water within an acceptable computational time. The initial coordinates of trehalose were obtained from the GlycoSciences Database (http://www.glycosciences.de/). Force field parameters and topology for trehalose molecules were generated using the PRODRG2 server (http://davapc1.bioch.dundee.ac.uk/cgi-bin/prodrg_beta) [29]. The peptide was first placed in a cubic box with periodic boundary conditions. The size of the cubic box throughout the simulations was roughly 80 Å with negligible volume fluctuations. Then, trehalose molecules (when included) were added into the box. The distances between solute molecules in 0.065 and 0.098 mol/L trehalose were at least 10 and 7 Å, respectively, which ensure an isotropic distribution of trehalose molecules around the peptide. Thereafter, water molecules non-overlapping with either the peptide or trehalose were randomly added in the simulation box. Finally, three positive ions (Na^+) were added by replacing the corresponding number of water molecules at the most negative electrical potential to achieve a neutral condition. At first, water and trehalose (if present) were minimized for 1000 steps keeping the peptide atoms fixed in their original positions. Next, the peptide alone was minimized for 1000 steps. Finally, the whole system was minimized for further 1000 steps. In order to allow for solvent relaxation, the system was subsequently equilibrated for about 100 ps with a constant number of particles (N), volume (V), and temperature (T), i.e., NVT ensemble, followed by further 100 ps at NPT conditions. The convergence of potential energy indicated equilibrium (data not shown). To make sure that the effects of trehalose on the peptide folding in different trehalose concentrations is the intrinsic character of trehalose rather than a stochastic output of simulations, six to eight MD simulations of 20 ns were conducted for each system at a constant trehalose concentration (0–0.26 mol/L) under different initial conditions by assigning different initial velocities on each atom of the simulation systems. Table 1 summarizes some simulation data for the different systems in the present study.

2.3. Analyses

The simulation trajectories were analyzed using several auxiliary programs provided with the GROMACS package. The programs include g_rms for the comparison of any two structures by computing the root-mean-square deviation (RMSD), g_gyrate for the radius of gyration (Rg) of the peptide, and g_hbond for the H-bond interactions between hydrogen donors and acceptors. H-bonds are considered to be intact if the donor-to-acceptor distance

Table 1
Compositions of simulated trehalose systems (one peptide molecule is used for all cases)

Trehalose concentration (mol/L)	Number of water	Number of trehalose molecules	Simulation length[a] (ns)
0	17046	0	20 (6)
0.065	16719	20	20 (8)
0.098	16558	30	20 (8)
0.13	16396	40	20 (6)
0.26	15788	80	20 (6)

[a] The number of repetitive simulation runs are given in parentheses.

is less than 3.5 Å and the donor-hydrogen-acceptor angle is within 30° of linearity.

The free energy surface is an important parameter for the understanding of the protein folding reaction. To explore the thermodynamics and kinetics of the peptide folding, we calculated the free energy as a function of the number of backbone H-bonds in the peptide conformation and the radius of gyration of the peptide. The corresponding free energy surface along an n-dimensional reaction coordinate $V = (v_1, v_2, \ldots v_n)$ is given by

$$\Delta G(V) = -k_B T(\ln P(V) - \ln P_{max}) \quad (1)$$

where $P(V)$ is the probability distribution obtained from a histogram, which are averaged over different trajectories under the same condition, and P_{max} denotes the maximum of the distribution, which is subtracted to ensure that $\Delta G = 0$ for the lowest free energy minimum. The weighted histogram analysis method (WHAM) is used to combine data and construct the free energy landscape [30].

Simulation trajectories were visualized, and three-dimensional figures were prepared using the Visual Molecular Dynamics (VMD) software [31].

3. Results and discussion

3.1. Properties of the peptide in different solvent environments

Starting from the fully extended peptide, we conducted 34 sets of 20 ns MD simulations (Table 1). Similar features were observed in all sets of the MD simulations in the same trehalose solution, although each simulation has started from different unbiased initial conditions. To avoid obtaining non-representative results, the simulations for the peptide in different trehalose concentrations were performed in parallel six to eight times, as shown in Table 1. First, two parameters, the RMSD from the initial structure for Cα atoms and the peptide Rg, are used to represent the conformational changes of the peptide during the folding. The Cα RMSD and Rg are displayed as a function of time in Fig. 1(a) and (b), respectively. It can be seen from Fig. 1(a) that the Cα RMSD values in trehalose solutions increase more rapidly than that in water at the initial stage, and they all essentially approach stable values after 2 ns. At the cases in trehalose solutions, the final values of the Cα RMSD decrease with increasing the concentration of trehalose, and they are smaller than that in pure water, except the one in 0.065 mol/L trehalose solution (the molar ratio of trehalose to peptide is 20). In addition, the values of Rg in 0.065 mol/L trehalose solution become stable at a time no more than 1.82 ns, much faster than that in water (5.2 ns). At the three high trehalose concentrations (0.098–0.26 mol/L), however, the Rg value of the native peptide is not reached. The results depicted above implicate that trehalose facilitate the peptide folding in 0.065 mol/L trehalose solution, whereas it inhibits the folding to some extent at higher trehalose concentrations. Such a behavior is qualitatively consistent with the experimental observation of firefly luciferase refolding in the presence of trehalose [10].

3.2. Peptide folding affected by trehalose molecules

Analyses of the Cα RMSD and Rg data (Fig. 1) have revealed the facilitated folding behavior of the peptide in 0.065 mol/L trehalose solution. To view the molecular details, a series of snapshots obtained by one of the simulations illustrating the evolution of trehalose-assisted peptide folding are given in Fig. 2. At the beginning of the simulation, trehalose molecules are distributed homogeneously in the box, and there is only one trehalose molecule near the peptide (as indicated by the arrow in Fig. 2), which is within a distance of 8 Å from the peptide. The trehalose molecule quickly approaches the peptide molecule, expels some water molecules and occupies the position around the residues of Glu 5, Ser 6, Ser 7, and Leu 8 (shown by green Licorice), where a β-turn forms (Fig. 2(a)). After 0.605 ns, the trehalose molecule bridges the two strands by hydrogen bonding and facilitates the formation of the β-turn (Fig. 2(b)). It corresponds well to the sharp decrease of the Rg value at about 0.6 ns (Fig. 1(b)). It is considered that the interactions between the two strands are stronger than those between the peptide and trehalose, so the trehalose molecule is gradually removed from between the two strands, and an H-bond is formed between the amide hydrogen of Leu 8 and the carbonyl oxygen of Glu 5 (Fig. 2(c)). At the moment, the peptide is surrounded by the other three trehalose molecules. When the turn structure is formed, the H-bonds between the two strands start to form near the turn. At 0.97 ns, the trehalose molecule slides away from the interspace of the two strands, and fluctuates around the peptide as shown in Fig. 2(d). In the following time, the peptide rearranges slightly until 1.82 ns to form a stable β-hairpin (Fig. 2(e)). Without trehalose, however, the peptide folding is only driven by intra-peptide interactions [32]. It can be seen from Fig. 1(a) that RMSD of the peptide increases before about 1.37 ns. The conformation of the peptide visualized by VMD software at 1.37 ns shows that the two strands of the peptide collapse toward a compact structure. It is over two times longer than that in 0.065 mol/L trehalose. In addition, the peptide needs to rearrange to its native structure until 5.2 ns in the absence of trehalose (Fig. 1(b)), while a stable structure has been kept since

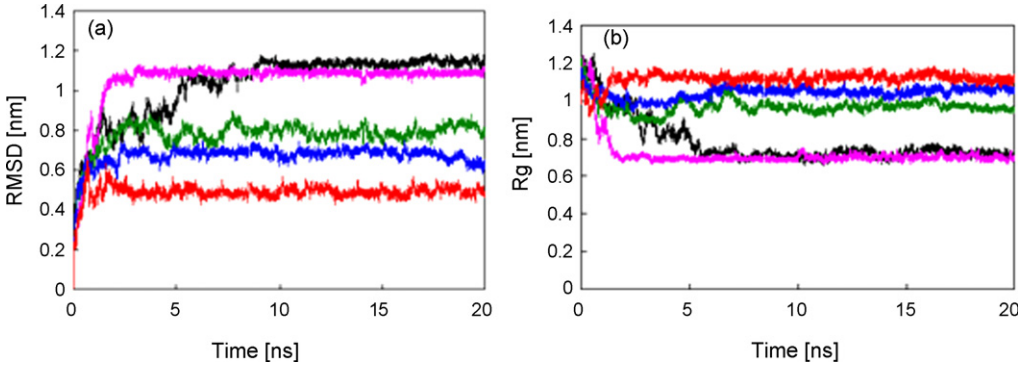

Fig. 1. (a) Root-mean-square atomic positional deviation (RMSD) (average of all parallel simulations in the same trehalose concentration) from the initial structure for Cα atoms and (b) radius of gyration (Rg) (average of all parallel simulations in the same trehalose concentration) as a function of time for the simulations in the absence (black) and presence of 0.065 mol/L (pink), 0.098 mol/L (green), 0.13 mol/L (blue), 0.26 mol/L (red) trehalose.

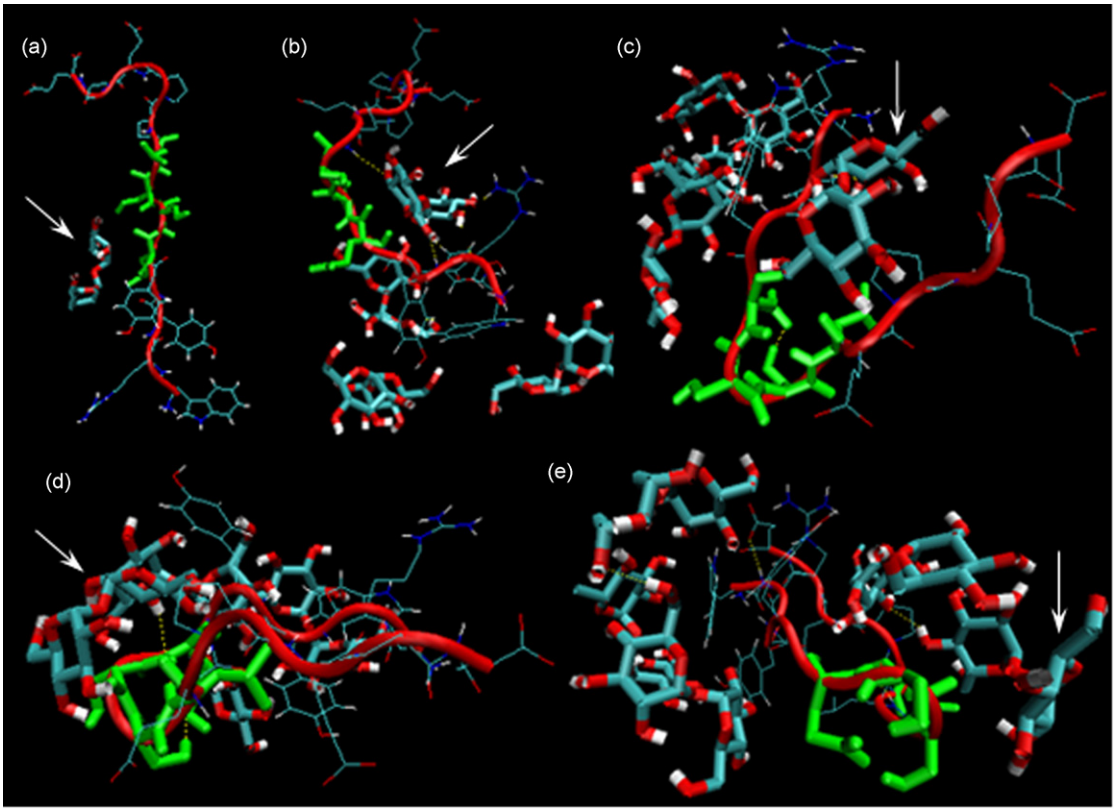

Fig. 2. Snapshots of MD simulations of the peptide folding in the presence of 0.065 mol/L trehalose at (a) 0.001 ns, (b) 0.605 ns, (c) 0.839 ns, (d) 0.97 ns, and (e) 1.82 ns. The residues (Glu 5, Ser 6, Ser 7 and Leu 8) involved in the turn are shown by green Licorice. The backbone and side chains of the other residues are shown by a red tube and thin sticks, respectively. The trehalose molecule which helps the peptide folding is indicated by the arrow. Trehalose molecules are shown by DynamicBonds. Hydrogen bonds are marked by dotted-yellow lines. Atoms are colored red for oxygen, blue for nitrogen, white for hydrogen, and green for carbon. All the structures in this article are plotted with the visual molecular dynamics (VMD) software (http://www.ks.uiuc.edu/Research/vmd/).

1.82 ns in 0.065 mol/L trehalose (Figs. 1(b) and 2(e)). Hence, in the proper trehalose concentration (0.065 mol/L), the peptide folds faster than in the solution without trehalose.

When the peptide folding is performed in trehalose higher than 0.065 mol/L, however, the inhibition effect of trehalose molecules on the β-hairpin folding is observed (Fig. 1). Fig. 3 contains four snapshots for the evolution of the peptide folding in 0.098 mol/L trehalose (the molar ratio of trehalose to peptide is 30). As shown in Fig. 3(a), there are four trehalose molecules near the peptide in the starting solution, which is within a distance of 8 Å from the peptide. This value is four times larger than that in 0.065 mol/L trehalose. It is considered due to the interactions between the peptide and trehalose molecules, making that the distribution of trehalose around the peptide does not correspond to the trehalose–peptide ratios as in 0.065 mol/L trehalose. After 0.4 ns, a trehalose molecule approaches the C-terminal of the peptide, making it more flexible and bend to the other strand. Meanwhile, another trehalose molecule approaches the peptide and forms two H-bonds with the peptide (Fig. 3(b)). Then, at 2 ns the two trehalose molecules interact with each other by hydrogen bonding, and are enveloped inside the peptide by hydrogen bonding (Fig. 3(c)). Finally, four trehalose molecules cluster and are remained in the peptide region after 4.68 ns (Fig. 3(d)). The result suggests that a lot of H-bonds can form between the peptide and trehalose molecules, so the intra-molecular interactions of the peptide backbone cannot compete with the interactions between the peptide and trehalose. It is likely the reason for the inhibition effect of trehalose at high concentrations. Similar phenomena are observed in 0.13 and 0.26 mol/L trehalose solutions.

3.3. Free energy landscapes of the peptide folding

A wealth of information on the folding mechanism can be extracted from the free energy landscapes of the peptide folding. With the free energy landscape, it is possible to evaluate the relative stability of a peptide in different states and, to some extent, to help us calculate the difference in free energy between the folded and the intermediate states. Several researchers have shown that the number of backbone H-bonds and Rg play an important role in elucidating the folding process of the β-hairpin peptide [33,34]. Hence, we constructed two-dimensional profiles from the simulation using the backbone H-bonds and Rg as the reaction coordinates in different trehalose solutions. For clarity, the inhibition effect of trehalose on the peptide folding is only discussed using 0.098 mol/L trehalose.

Fig. 4 shows the free energy landscapes projected to the reaction coordinates the numbers of backbone H-bonds and Rg in water (a), and in 0.065 mol/L trehalose (b). It is observed from Fig. 4 that in both the solutions there are four energy minima in the free energy landscapes, so the folding process can be divided into four states: three intermediate states I_1, I_2 and I_3, and folded state F, which appears in the global energy minimum. Here, we first characterize the properties of these states according to their positions on the energy landscapes. Table 2 shows the population of each state, the mean number of backbone H-bonds, and the mean radius of gyration of the peptide. The F state is composed of conformations with a compact structure (Rg ≈ 0.7 nm) and about two backbone H-bonds. The I_3 state remains an Rg similar to the F state, but the number of backbone H-bonds is quite different (it has only zero to one backbone H-bond). Although both the I_1 and I_2

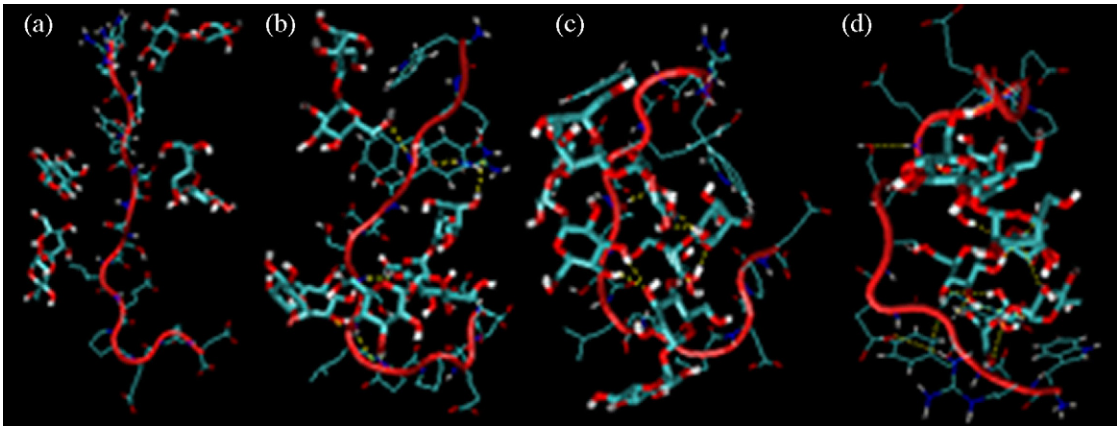

Fig. 3. Snapshots of MD simulations of the peptide folding in the presence of 0.098 mol/L trehalose at (a) 0.001 ns, (b) 0.4 ns, (c) 2 ns, and (d) 4.68 ns. The illustrations are the same as those described in the caption to Fig. 2.

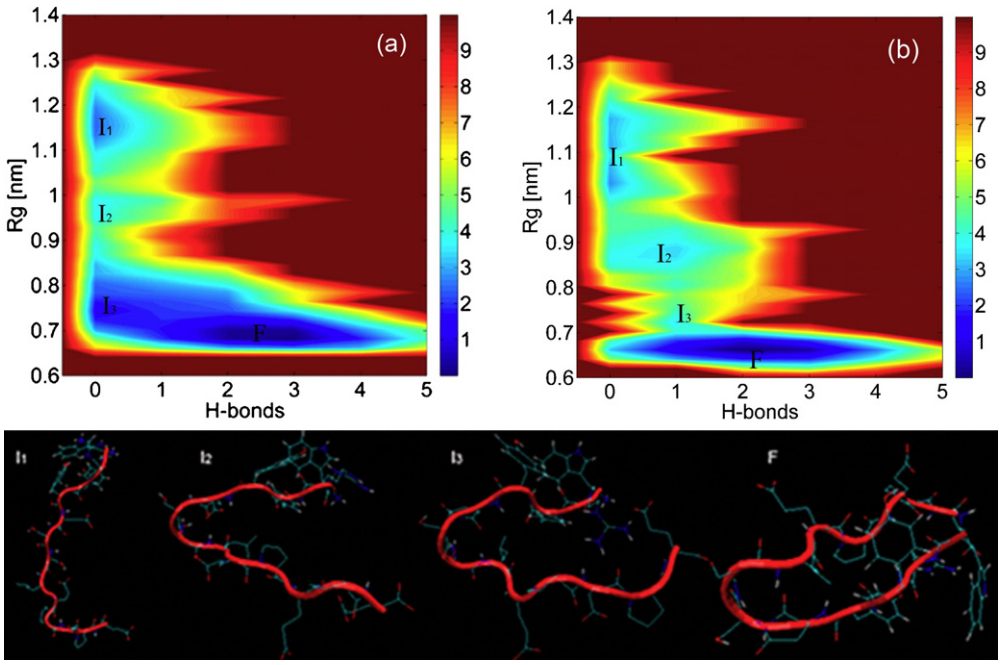

Fig. 4. Free energy profiles versus the number of the backbone hydrogen bonds (H-bonds) and the radius of gyration (Rg) of the peptide in water (a) and in 0.065 mol/L trehalose (b). The intermediate (I_1, I_2, and I_3) and folded (F) states are marked in the pictures, the configurations of the most populated clusters within the basins of I_1, I_2, I_3 and F states are given in the bottom panel. Images were generated using the visual molecular dynamics (VMD) software. The illustrations in the bottom panel are the same as those described in the caption to Fig. 2.

states do not have any backbone H-bonds, the mean Rg value of the I_2 state is smaller than that of I_1 state. In terms of the mean backbone dihedral angles shown in Table 3, the structures of the three residues (Ser 6, Ser 7, and Leu 8) at the turn change greatly during the peptide folding from I_1 to I_3 state. This is more significant for the ψ angles. In the transitions, however, the remaining residues maintain a similar conformation (β-sheet structure) (Table 3). In the transition from I_3 to F state, the mean backbone dihedral angles change little, so it can be concluded that the turn has almost formed correctly in the I_3 state.

Although the free energy contours shown in Fig. 4(a) and (b) have a similar shape, there is a notable difference in the population of the I_3 and F states, as shown in Table 2. The population of the F state (74%) in 0.065 mol/L trehalose is over twice higher than that in water. The large population of the F state further makes us believe that the peptide folding is facilitated by trehalose molecules in 0.065 mol/L trehalose. Although the I_1 and I_2 states in both the solutions have similar populations, the amount of the I_3 state in 0.065 mol/L trehalose is about 20 times less than that in water (Table 2). It indicates that trehalose can interact with the F state, and stabilize it, thereby leading to an equilibrium shift from I_3 toward F state. Hence, the MD simulation reveals that the transition from I_3 to F state is induced in 0.065 mol/L trehalose. However, trehalose at this concentration does not change the folding pathway (Fig. 4), which agrees with that observed by Chen et al. [35] in the study of ribosomal protein S6 refolding in trehalose solutions.

In contrast to the above results, when the peptide folding is simulated in 0.098 mol/L trehalose solution, only three local minima are observed in the free energy landscape (Fig. 5), corresponding to intermediate I_1 (Rg ≈ 1.17 nm), I_2 (Rg ≈ 1.09 nm) nm) and misfolded (M) (Rg ≈ 0.89 nm, or 0.8 nm < Rg < 1.0 nm as observed in Fig. 5) states. It is noted that the I_1 state has quite similar properties to that in 0.065 mol/L trehalose solution

Table 2
Comparison of the conformational states of the peptide as revealed by the free energy surfaces displayed in Figs. 4 and 5

	State				
	I_1	I_2	I_3	F	M
Water					
Population (%)	12.1	2.1	41.3	34.6	NA
⟨H-bonds⟩	0 (0)	0 (0)	0.7 (0.8)	2.3 (0.7)	NA
⟨Rg⟩ (nm)	1.17 (0.04)	0.98 (0.02)	0.77 (0.03)	0.70 (0.01)	NA
0.065 mol/L trehalose					
Population (%)	10.2	4.5	2.1	74	NA
⟨H-bonds⟩	0 (0)	0.6 (0.5)	0.9 (0.2)	2.1 (0.8)	NA
⟨Rg⟩ (nm)	1.10 (0.05)	0.89 (0.02)	0.74 (0.02)	0.69 (0.01)	NA
0.098 mol/L trehalose					
Population (%)	1.22	2.45	NA	NA	95.4
⟨H-bonds⟩	0 (0)	0 (0)	NA	NA	0.7 (0.7)
⟨Rg⟩ (nm)	1.17 (0.02)	1.09 (0.02)	NA	NA	0.89 (0.03)

⟨H-bonds⟩ represents the mean number of peptide backbone H-bonds, ⟨Rg⟩ the mean radius of gyration. Standard deviations from the mean values are given in parentheses. NA, not applicable. All of the trajectories in the same trehalose concentration were used to compute the above parameters.

(Table 2). However, the M state does not have a compact structure (0.8 nm < Rg < 1.0 nm) as the F state does (Rg ≈ 0.7 nm), and it has only zero to one backbone H-bonds. The sum of the populations of the I_1 and I_2 states is only about 3.6%, while the M state has an overwhelming population (95.4%). It suggests that, at the beginning, the peptide folding is facilitated by trehalose in 0.098 mol/L trehalose solution, which corresponds well to the sharp decrease of the Rg value at about 0.6 ns (Fig. 1(b)). But the peptide gets rapidly trapped in a local free energy basin under the condition, forming a stable misfolded state.

In terms of the transition state theory of reaction kinetics, protein folding rate is determined by the values of free energy barrier [36]. From the free energy profile, we can locate the position of the energy barrier by free energy optimization in the reaction coordinate space. Then, we can calculate the value of the free energy at the location of the transition state, which determine all the energy barrier heights from the initial conformation to the native state. To illustrate the variation of the free energy barriers in different trehalose solutions, one-dimensional free energy curves of the peptide folding at different trehalose concentrations along the RMSD are shown in Fig. 6. To obtain the free energy from the RMSD, the peptide structures sampled every 0.5 ps were collected and projected onto 20 grid cells used to divide the overall accessible range. For every cell, the number of points was counted and the relative probability density was calculated. Finally, the grid cell with the highest probability was chosen as the reference state, i.e., the cell corresponding to the overall free energy minimum, and free energy landscape was obtained from Eq. (1). The WHAM method was used to combine data and calculate the minimum free energy path. It is clear in Fig. 6 that four minima are discovered in water, in well correspondence with that shown in Fig. 4(a): the first one (I_1) at RMSD = 3.4 Å, the second one (I_2) at RMSD = 6.1 Å, the third one (I_3) at RMSD = 10 Å and the last one (F) at RMSD = 11 Å. The first two minima are separated by an energy barrier of approximately 1.4 k_BT, and the potential energy barrier between the I_2 and I_3 states is 2.5 k_BT. However, there is only a minor energy barrier (0.3 k_BT) between the I_3 and F states. It indicates that the peptide first needs to cross two large potential energy barriers to fold from the I_1 state to I_3 state, and then it folds quickly to the F state.

Similar to the folding in pure water, the free energy landscape of the peptide folding in 0.065 mol/L trehalose solution also shows three potential energy barriers separating four energy minima. As compared to those in water, however, these energy barriers are much smaller. For example, the biggest potential energy barrier existing between I_2 (RMSD = 7.1 Å) and I_3 (RMSD = 9.3 Å) states is only 1.8 k_BT, less than that in water (2.5 k_BT). Hence, the peptide assisted by trehalose molecules can easily cross them and folds into the β-hairpin because the free energy barriers between the four states decrease greatly in 0.065 mol/L trehalose solution. In other words, the peptide folds much faster in 0.065 mol/L trehalose solution than in pure water, so the first three states are short-lived in 0.065 mol/L trehalose solution.

In the case of the peptide folding in 0.098 mol/L trehalose solutions, the free energy landscape shows only three local minimum values at RMSD values of 1.7, 4.1 and 7.7 Å. Although the first two free energy barriers are smaller than those in water, there is a huge free energy barrier, which is unable to conquer, between the I_2 and M states. So, the peptide falls into a deep local free energy trap and cannot jump out of it.

Table 3
Comparison of the mean dihedral angles (ϕ, ψ) in degrees of the main conformational states obtained from Fig. 4

	State			
	I_1	I_2	I_3	F
Trp1	−25, 140	−14, 139	5, 136	4, 137
Arg2	−107, 123	−118, 133	−128, 139	−120, 146
Tyr3	−94, 127	−82, 122	−77, 118	−84, 101
Tyr4	−119, 106	−113, 111	−105, 110	−107, 90
Glu5	−112, 123	−106, 126	−122, 114	−134, 135
Ser6	−118, 114	−96, 74	−59, −38	−54, −40
Ser7	−100, 112	−117, 42	−69, −41	−78, −40
Leu8	−97, 101	−90, 81	−67, −48	−93, −69
Glu9	−98, 114	−87, 113	−124, 98	−127, 106
Pro10	−57, −52	−57, −61	−60, −57	−83, 61
Glu11	−93, 113	−111, 107	−110, 112	−108, 106
Pro12	−66, 60	−61, 122	−65, 133	−66, 114
Asp13	−121, 61	−105, 40	−117, 117	−108, 74

All of the trajectories in the same trehalose concentration were used to compute the above parameters.

3.4. Analysis of peptide folding via H-bond interactions

The H-bonds involved in three different trehalose solutions (0, 0.065 and 0.098 mol/L) are analyzed. Table 4 lists the total number of inter-molecular H-bonds for various conformational states in different trehalose solutions. It has been known that peptide backbone H-bonds increase during the peptide folding [37]. The peptide backbone H-bonds are closely connected during the peptide desolvation because H-bonds between water and the peptide amidogen and carboxyl groups must be broken before the peptide backbone H-bonds can be formed. Daidone et al. [38] found

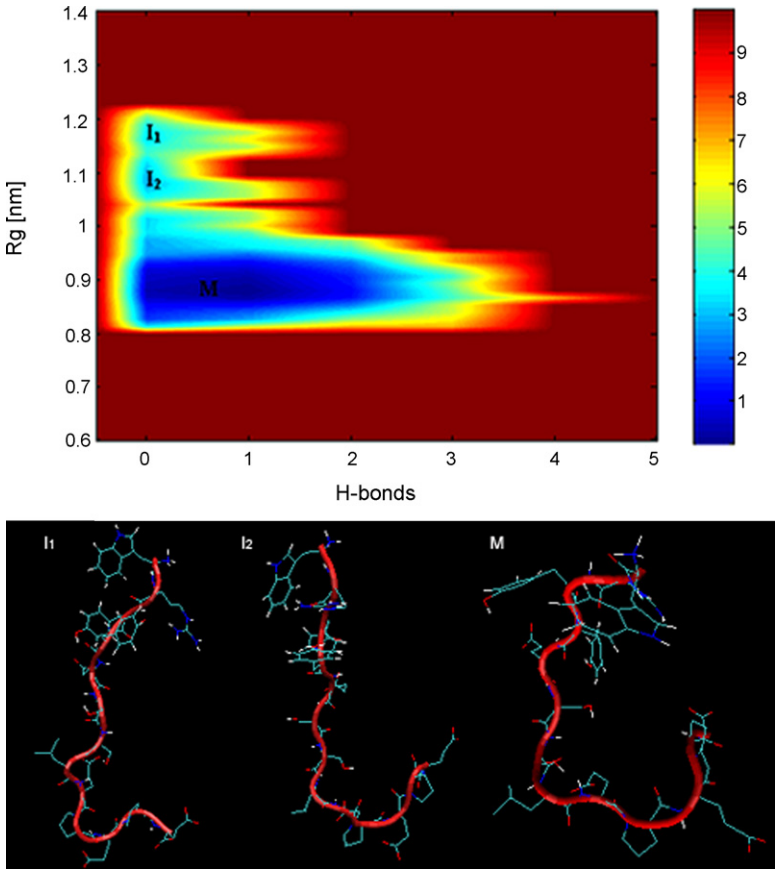

Fig. 5. Free energy profile versus the number of the backbone hydrogen bonds (H-bonds) and the radius of gyration (Rg) of the peptide in 0.098 mol/L trehalose. The intermediate (I_1 and I_2) and misfolded (M) states are marked in the figure. The configurations of the most populated conformations within the basins of I_1, I_2, and M states are given in the bottom panel. The illustrations in the bottom panel are the same as those described in the caption to Fig. 2.

that peptide desolvation is a driving force in the peptide folding. In 0.065 mol/L trehalose, some water molecules are excluded by trehalose molecules, and released to the bulk, as indicated by the decrease in the number of H-bonds between water and the peptide in the folding process (Table 4). Although the number of peptide-water H-bonds in the I_1 state in 0.065 mol/L trehalose is similar to that in water, the number of peptide-water H-bonds in the other three states decreases more greatly than in water (Table 4). This indicates that trehalose facilitates the peptide desolvation, so the folding rate is increased in the presence of 0.065 mol/L trehalose. This observation suggests that the disaccharide molecules accumulate around the peptide and partly exclude water, favoring the formation of intramolecular H-bonds and promoting the formation of secondary structures. In addition, it can be seen from Table 4 that the number of peptide-trehalose H-bonds increases somewhat during the folding from I_1 to F state in 0.065 mol/L trehalose. There are about two H-bonds between the peptide and trehalose in the F state in the presence of 0.065 mol/L trehalose, which is comparable to the number of the backbone H-bonds of the F state shown in Table 2. It is considered to be a favorable balance between the backbone H-bonds and the peptide-trehalose H-bonds; the favorable balance stabilizes the folded peptide.

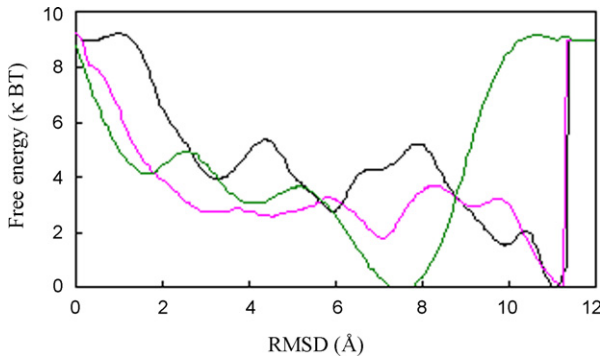

Fig. 6. The free energy as a function of root-mean-square atomic positional deviation (RMSD) from the initial structure for Cα atoms in different trehalose solutions (black, water; purple, 0.065 mol/L trehalose; green, 0.098 mol/L trehalose).

The changes of peptide-trehalose and water–peptide H-bonds in 0.098 mol/L trehalose have a similar tendency to that in 0.065 mol/L trehalose, but much more H-bonds are formed between the peptide and trehalose, and the number of peptide-trehalose H-bonds increases rapidly during the early folding stages in 0.098 mol/L trehalose solution (Table 4). Finally, over three H-bonds can form between the peptide and trehalose in the M state. Too many H-bonds between the peptide and trehalose inhibit the formation of the peptide backbone H-bonds (there is only zero to one peptide backbone H-bond in the M state, as shown in Table 2), so the peptide cannot fold into its native state in this high-concentration trehalose solution.

As trehalose concentration increases in the studied solutions, more trehalose–trehalose interactions occur (Table 4). For example, there are about 24 H-bonds between trehalose molecules in the M state in 0.098 mol/L trehalose. This is because most of the trehalose molecules cluster each other in the simulation system (data not shown). It is found that there are four trehalose

Table 4
Mean numbers of inter-molecular hydrogen bonds as a function of conformational states in different trehalose solutions

	State				
	I_1	I_2	I_3	F	M
Number of hydrogen bonds					
Pure water					
Water–peptide	63.8 (4.1)	64.1 (3.9)	59.4 (4.8)	54.3 (4.0)	NA
0.065 mol/L trehalose					
Water–peptide	63.4 (4.0)	62.8 (4.3)	56.2 (6.3)	44.7 (3.9)	NA
Trehalose–peptide	0.1 (0.4)	0.1 (0.3)	1.5 (1.2)	2.1 (1.3)	NA
Trehalose–trehalose	5.3 (3.3)	6.7 (2.6)	9.6 (4.5)	15.6 (5.4)	NA
0.098 mol/L trehalose					
Water–peptide	57.7 (4.4)	53.6 (3.8)	NA	NA	53.7 (4.3)
Trehalose–peptide	1.2 (1.0)	1.8 (1.2)	NA	NA	3.4 (1.6)
Trehalose–trehalose	6.8 (4.0)	7.0 (4.2)	NA	NA	24.0 (8.1)

H-bonds are considered to be intact when donor and acceptor atoms are within 3.5 Å and 30° of linearity. The conformations of the five states (I_1, I_2, I_3, F, and M) are identified using the program g_cluster implemented in the GROMACS molecular dynamics software package. It uses algorithm as described by Daura et al. [39]. The conformations are clustered by using a RMSD cutoff of 1 Å. Standard deviations from the mean values are given in parentheses. NA, not applicable. All of the trajectories in the same trehalose concentration were used to compute the above parameters.

molecules for which the distance between the heavy atom of trehalose and the peptide atoms is less than 8 Å. The four trehalose molecules surround the peptide and form a continuous space-filling network. Consequently, more H-bonds can form between the peptide and trehalose molecules when the peptide folds in the presence of higher trehalose concentrations. The inter-molecular H-bonds stabilize the M state and make it trapped in a local free energy basin. Namely, at high trehalose concentration the peptide folding is inhibited by direct interaction between the peptide and trehalose.

The above discussion seems inconsistent with the preferential exclusion theory for a protecting osmolyte such as trehalose, which depicts that the osmolyte raises the free energy of an unfolded peptide due to its unfavorable interaction with the peptide backbone [12,40]. However, it should be noted that the preferential exclusion mechanism does not deny the presence of the interactions between osmolyte polar groups and an unfolded peptide [40]. Moreover, our simulations are performed in low trehalose concentrations (0.065–0.26 mol/L), so the transfer free energy of the peptide is quite low, e.g., about 5.3 cal/mol at 0.098 mol/L trehalose, as estimated by linear extrapolation with the data reported previously [12,40]. In such a circumstance, the molecular interactions between the peptide and trehalose molecules would dominate the folding process.

4. Conclusions

In this article, we investigated the effect of trehalose on the β-hairpin peptide folding by MD simulation using an all-atom model. We have found that trehalose concentration greatly affects the peptide folding. At a proper trehalose concentration (0.065 mol/L), the peptide folds faster than that in water, but it cannot fold to the β-hairpin at higher trehalose concentrations. It was confirmed that in 0.065 mol/L trehalose solution, a trehalose molecule approaches the peptide, expels the water molecules, and makes the peptide significantly floppy. It is achieved by bridging between the two strands via H-bonds, which facilitates the peptide to collapse. The local potential energy barriers are reduced from the intermediate states to the native state. Thus, the peptide folding is facilitated. At this trehalose concentration, there is a favorable balance between the peptide backbone H-bonds and the inter-molecular H-bonds between peptide and trehalose, so the folded peptide is stabilized in the trehalose solution. At higher trehalose concentrations, however, many trehalose molecules are observed to cluster around the peptide, forming more H-bonds between the peptide and trehalose. So, the peptide is stabilized at a misfolded state and trapped in the local free energy basin. Thus, the molecular mechanisms of the facilitation and inhibition effects of trehalose on the β-hairpin folding have been clearly elucidated by the MD simulation.

Acknowledgments

This work was supported by the Natural Science Foundation of China (No. 20636040, 20676098) and the Natural Science Foundation of Tianjin from Tianjin Municipal Science and Technology Commission (Contract No. 08JCZDJC17100).

References

[1] J. Rösgen, Molecular basis of osmolyte effects on protein and metabolites, Methods Enzymol. 428 (2007) 459–486.
[2] D.W. Bolen, I.V. Baskakov, The osmophobic effect: natural selection of a thermodynamic force in protein folding, J. Mol. Biol. 310 (2001) 955–963.
[3] B.J. Bennion, V. Daggett, Counteraction of urea-induced protein denaturation by trimethylamine N-oxide: a chemical chaperone at atomic resolution, Proc. Natl. Acad. Sci. U.S.A. 101 (2004) 6433–6438.
[4] X.Y. Dong, Y. Huang, Y. Sun, Refolding kinetics of denatured-reduced lysozyme in the presence of folding aids, J. Biotechnol. 114 (2004) 135–142.
[5] S. Bourot, O. Sire, A. Trautwetter, T. Touzé, L.F. Wu, C. Blanco, T. Bernard, Glycine betaine-assisted protein folding in a *lysA* mutant of *Escherichia coli*, J. Biol. Chem. 275 (2000) 1050–1056.
[6] L.Y. Chen, J.A.B. Ferreira, S.M.B. Costa, G.J.M. Cabrita, D.E. Otzen, E.P. Melo, Compaction of ribosomal protein S6 by sucrose occurs only under native conditions, Biochemistry 45 (2006) 2189–2199.
[7] L. Cordone, G. Cottone, S. Giuffrida, G. Palazzo, G. Venturoli, C. Viappiani, Internal dynamics and protein–matrix coupling in trehalose-coated proteins, Biochim. Biophys. Acta 1749 (2005) 252–281.
[8] A.B. Richards, S. Krakowka, L.B. Dexter, H. Schmid, A.P.M. Wolterbeek, D.H. Waalkens-Berendsen, A. Shigoyuki, M. Kurimoto, Trehalose: a review of properties, history of use and human tolerance, and results of multiple safety studies, Food Chem. Toxicol. 40 (2002) 871–898.
[9] E.P. Melo, L. Chen, J.M. Cabral, P. Fojan, S.B. Petersen, D.E. Otzen, Trehalose favors a cutinase compact intermediate off-folding pathway, Biochemistry 42 (2003) 7611–7617.
[10] M.A. Singer, S. Lindquist, Multiple effects of trehalose on protein folding in vitro and in vivo, Mol. Cell 1 (1998) 639–648.
[11] S.D. Allison, B. Chang, T.W. Randolph, J.F. Carpenter, Hydrogen bonding between sugar and protein is responsible for inhibition of dehydration-induced protein unfolding, Arch. Biochem. Biophys. 365 (1999) 289–298.
[12] M. Auton, D.W. Bolen, Additive transfer free energies of the peptide backbone unit that are independent of the model compound and the choice of concentration scale, Biochemistry 43 (2004) 1329–1342.
[13] C.D. Snow, E.J. Sorin, Y.M. Rhee, V.S. Pande, How well can simulation predict protein folding kinetics and thermodynamics? Annu. Rev. Biophys. Biomol. Struct. 34 (2005) 43–69.
[14] L. Mirny, E. Shakhnovich, Protein folding theory: from lattice to all-atom models, Annu. Rev. Biophys. Biomol. Struct. 30 (2001) 361–396.

[15] B.J. Bennion, V. Daggett, The molecular basis for the chemical denaturation of proteins by urea, Proc. Natl. Acad. Sci. U.S.A. 100 (2003) 5142–5147.
[16] S. Gnanakaran, H. nymeyer, J. Portman, K.Y. Sanbonmatsu, A. García, Peptide folding simulations, Curr. Opin. Struct. Biol. 13 (2003) 168–174.
[17] J. Khandogin, J. Chen, C.L. Brooks III, Exploring atomistic details of pH-dependent peptide folding, Proc. Natl. Acad. Sci. U.S.A. 103 (2006) 18546–18550.
[18] G. Wei, N. Mousseau, P. Derreumaux, Complex folding pathways in a simple β-hairpin, Proteins 56 (2004) 464–474.
[19] B. Ma, R. Nussinov, Energy landscape and dynamics of the β-hairpin G peptide and its isomers: topology and sequences, Protein Sci. 12 (2003) 1882–1893.
[20] J. Zhang, M. Qin, W. Wang, Folding mechanism of beta-hairpins studied by replica exchange molecular simulations, Proteins 62 (2006) 672–685.
[21] D. van der Spoel, E. Lindahl, B. Hess, G. Groenhof, A.E. Mark, H.J.C. Berendsen, GROMACS: fast, flexible, and free, J. Comput. Chem. 26 (2005) 1701–1718.
[22] W.F. van Gunsteren, S.R. Billeter, A.A. Eising, P.H. Hünenberger, P. Krüger, A.E. Mark, W.R.P. Scott, I.G. Tironi, Biomolecular Simulation: The GROMOS96 Manual and User Guide, Hoschsulverlag AG an der Zurich, Zürich, Switzerland, 1996 .
[23] H.J.C. Berendsen, J.P.M. Postma, W.F. van Gunsteren, J. Hermans, Interaction models for water in relation to protein hydration, in: B. Pullman (Ed.), Intermolecular Forces, D Reidel Publishing Company, Dordrecht, 1981, pp. 331–342.
[24] T. Darden, D. York, L. Pedersen, Particle mesh Ewald: an *N·log(N)* method for Ewald sums in large systems, J. Chem. Phys. 98 (1993) 10089–10092.
[25] B. Hess, H.J.C. Berendsen, J.G.E.M. Fraaije, LINCS: a linear constraint solver for molecular simulations, J. Comput. Chem. 18 (1997) 1463–1472.
[26] L. Verlet, Computer "experiments" on classical fluids. I. Thermodynamical properties of Lennard-Jones molecules, Phys. Rev. 159 (1967) 98–103.
[27] H.J.C. Beredsen, J.P.M. Postma, W.F. van Gunsteren, A. Di Nola, J.R. Haak, Molecular dynamics with coupling to an external bath, J. Chem. Phys. 81 (1984) 3684–3690.
[28] A.S.N. Seshasayee, K. Raghunathan, K. Sivaraman, G. Pennathur, Role of hydrophobic interactions and salt-bridges in β-hairpin folding, J. Mol. Model. 12 (2006) 197–204.
[29] A.W. Schuettelkopf, D.M.F. van Aalten, PRODRG: a tool for high-throughput crystallography of protein–ligand complexes, Acta Crystallogr. D 6 (2004) 1355–1363.
[30] S. Kumar, J.M. Rosenberg, D. Bouzida, R.H. Swendsen, P.A. Kollman, The weighted histogram analysis method for free-energy calculations on biomolecules. I. The method, J. Comput. Chem. 13 (2004) 1011–1021.
[31] W. Humphrey, A. Dalke, K. Schulten, VMD: visual molecular dynamics, J. Mol. Graphics 14 (1996) 33–38.
[32] J. Chen, W. Im, C.L. Brooks III, Balancing solvation and intramolecular interactions: toward a consistent generalized Born force field, J. Am. Chem. Soc. 128 (2006) 3728–3736.
[33] R. Zhou, Exploring the protein folding free energy landscape: coupling replica exchange method with P3ME/RESPA algorithm, J. Mol. Graphics Model. 22 (2004) 451–463.
[34] P.H. Nguyen, G. Stock, E. Mittag, C.K. Hu, M.S. Li, Free energy landscape and folding mechanism of a β-hairpin in explicit water: a replica exchange molecular dynamics study, Proteins 61 (2005) 795–808.
[35] L.Y. Chen, G.J.M. Cabrita, D.E. Otzen, E.P. Melo, Stabilization of the ribosomal protein S6 by trehalose is counterbalanced by the formation of a putative off-pathway species, J. Mol. Biol. 351 (2005) 402–416.
[36] J.E. Shea, C.L. Brooks III, From folding theories to folding proteins: a review and assessment of simulation studies of protein folding and unfolding, Annu. Rev. Phys. Chem. 52 (2001) 499–535.
[37] S. Scheiner, Contributions of NH···O and CH···O hydrogen bonds to the stability of β-sheets in proteins, J. Phys. Chem. B 110 (2006) 18670–18679.
[38] I. Daidone, M.B. Ulmschneider, A.D. Nola, A. Amadei, J.C. Smith, Dehydration-driven solvent exposure of hydrophobic surfaces as a driving force in peptide folding, Proc. Natl. Acad. Sci. U.S.A. 104 (2007) 15230–15235.
[39] X. Daura, K. Gademann, B. Jaun, D. Seebach, W.F. van Gunsteren, A.E. Mark, Peptide folding: when simulation meets experiment, Angew. Chem. Int. Ed. 38 (1999) 236–240.
[40] T.O. Street, D.W. Bolen, G.D. Rose, A molecular mechanism for osmolyte-induced protein stability, Proc. Natl. Acad. Sci. U.S.A. 103 (2006) 13997–14002.